Ultralow-Dielectric-Constant Films Prepared from Hollow Polyimide Nanoparticles Possessing Controllable Core Sizes

Gufan Zhao,[†] Takayuki Ishizaka,*[,‡] Hitoshi Kasai,[†] Masatoshi Hasegawa,[§] Takeo Furukawa,[||] Hachiro Nakanishi,[†] and Hidetoshi Oikawa[†]

Institute of Multidisciplinary Research for Advanced Materials, Tohoku University, 2-1-1 Katahira, Aoba-ku, Sendai, Miyagi 980-8577, Japan, Research Center for Compact Chemical Process, AIST (National Institute of Advance Science and Technology), 4-2-1 Nigatake, Miyagino-ku, Sendai, Miyagi 983-8551, Japan, Department of Chemistry, Faculty of Science, Toho University, 2-2-1 Miyama, Funabashi, Chiba 274-8510, Japan, and Department of Chemistry, Faculty of Science, Tokyo University of Science, 1-3 Kagurazaka, Shinjuku-ku, Tokyo 162-8601, Japan

Received November 18, 2008

Polyimide (PI) is a candidate material that is showing promise for use in a wide range of applications in several advanced technologies. In this study, we employed the reprecipitation method and subsequent imidization to prepare unique hollow PI nanoparticles (NPs) by blending a suitable polymer porogen with the PI precursor in the form of individual NPs. The hollow structures were induced through phase separation between the PI and the porogen, a process that was influenced by the compatibility between the two polymers. We then assembled multilayered films by depositing the hollow PI NPs electrophoretically onto a substrate. After spin-coating a solution of the PI precursor and then subjecting the system to thermal treatment, the individual PI NPs were bound to their adjacent neighbors, thereby improving the film strength to some extent. We obtained dense, uniformly packed films having controlled thicknesses in the range from 500 nm to 10 μm. This strategy provided films in which air voids existed between and within the composite PI NPs; as a result, the dielectric constant reached as low as 1.9.

Introduction

One approach toward increasing the processing speeds of highly integrated circuits in computers is to develop dielectric materials possessing ultralow dielectric constants (ultralow-k: $k < 2.0$) as replacements for silicon dioxide, thereby reducing the capacitance between metal interconnects, the resistance−capacitance delay, line-to-line crosstalk noise, and power dissipation.[1] Although doping with carbon and introducing air pores both lower the dielectric constant of silicon dioxide, the mechanical strength decreases drastically. Polyimide (PI), a representative high-performance plastic, is among the most promising candidates for use as a next-generation interlayer dielectric;[2,3] indeed, it is already being employed as a flexible dielectric material in microelectronic devices. Recently, PI polymers exhibiting lower dielectric constants have been in demand for use in flexible printed circuits.

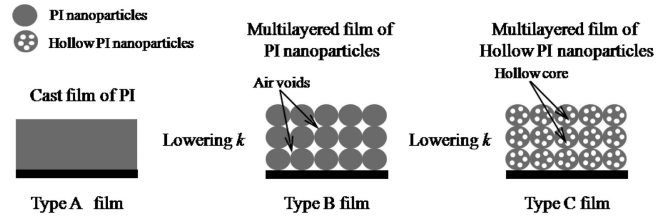

Figure 1. Schematic illustration of a simple strategy to reduce the dielectric constant (k) of PI films (Type A) by introducing air voids between PI NPs (Type B) and hollow cores into separate PI NPs (Type C).

Despite the many attempts at developing low-k PI films[4−12] of type A (Figure 1), including fluorinated PIs, semiaromatic PIs, and porous PI films, their dielectric constants have remained relatively high ($k = 2.4−3.0$). We have proposed the deposition of PI nanoparticles (NPs) onto a substrate as an alternative approach toward the preparation of low-k ($k < 2.5$) PI films (Type B films, Figure 1), that is, by introducing air voids ($k = 1$) between the PI NPs.[13] To further reduce their dielectric constants, we have focused on

* To whom correspondence should be addressed. Phone: +81-22-237-2098. Fax: +81-22-237-5215. E-mail: t-ishizaka@aist.go.jp.
[†] Tohoku University.
[‡] AIST (National Institute of Advance Science and Technology).
[§] Toho University.
[||] Tokyo University of Science.

(1) International Technology Roadmap for Semiconductors. http://www.itrs.net (accessed Mar 2008).
(2) Maier, G. *Prog. Polym. Sci.* **2001**, *26*, 3–65.
(3) Hasegawa, M.; Horie, K. *Prog. Polym. Sci.* **2001**, *26*, 259–335.
(4) Anderson, M. R.; Davis, R. M.; Taylor, C. D.; Parker, M.; Clark, S.; Marciu, D.; Miller, M. *Langmuir* **2001**, *17*, 8380–8385.
(5) Eichstadt, A. E.; Ward, T. C.; Bagwell, M. D.; Farr, I. V.; Dunson, D. L.; McGrath, J. E. *Macromolecules* **2002**, *35*, 7561–7568.
(6) Ando, S.; Matsuura, T.; Sasaki, S. *Macromolecules* **1992**, *25*, 5858–5860.
(7) Feiring, A. E.; Auman, B. C.; Wonchoba, E. R. *Macromolecules* **1993**, *26*, 2779–2784.
(8) Hasegawa, M.; Horiuchi, M.; Wada, Y. *High Perform. Polym.* **2007**, *19*, 175–193.
(9) Hasegawa, M. *High Perform. Polym.* **2001**, *13*, S93–S106.
(10) Hedrick, J. L.; Russel, T. P.; Labadie, J.; Lucas, M.; Swanson, S. *Polymer* **1995**, *36*, 2685–2697.
(11) Hedrick, J. L.; Miller, R. D.; Hawker, C. J.; Carter, K. R.; Volksen, W.; Yoon, D. Y.; Trollsås, M. *Adv. Mater.* **1998**, *10*, 1049–1053.
(12) Takeichi, T.; Arimatsu, K. *J. Photopolym. Sci. Technol.* **2001**, *14*, 67–72.

10.1021/cm802989u CCC: $40.75
Published on Web 12/29/2008

incorporating hollow cores into the individual PI NPs with the aim of assembling them into multilayered films (Type C films, Figure 1). This strategy should be a relatively simple and effective means of introducing air porosity uniformly into ultralow-k PI films, one that is comparable with the method used to prepare air gap structures through delicate synthesis of PI−porogen copolymers followed by decomposition of the block/graft porogen.[10,11] Unfortunately, we could not synthesize the desired hollow PI NPs using template-assisted emulsion/suspension polymerization because of the insolubility of PI in common solvents. Because the further incorporation of air into the films could lead to rapid deterioration of the mechanical properties of the PI films, it is necessary to find a compromise between their degree of porosity and the desired properties (e.g., dielectric constants).

Previously, we demonstrated that size-controlled PI NPs (diameters: 30−500 nm) could be produced using the reprecipitation method and subsequent imidization.[14,15] We have also prepared porous PI NPs possessing superficial pores by adding a second polymer, poly(acrylic acid) (PAS), as the porogen.[16] The porous structures in these systems result from microphase separation between poly(amic acid) (PAA, the precursor of PI) and the porogen; highly porous structures result when the two polymers are reasonably compatible. The compatibility of PAA and the porogen can be improved by varying the type of PAA, thereby making it possible to increase the depth of the pores, which are the remnants of the spherical porogen phases. Indeed, porogen phases on the surface of PAA remain the deepest[17] when using the most compatible combination of PAA and porogen. The compatibility between the polymers can be estimated from the solubility parameter[18] (δ) of each component: the closer the two solubility parameters, the more compatible the polymers. The small difference ($\Delta\delta$) between the solubility parameters of PAA ($\delta_{PAA} = 20.8$) and PAS ($\delta_{PAS} = 23.6$) provides superficial porous structures, whereas the larger $\Delta\delta$ between PAA ($\delta = 20.8$) and poly(vinyl alcohol) ($\delta_{PVAL} = 30.5$) provides an almost nonporous structure because of ejection of the porogen from the PAA particles.[16]

Here, we present a novel strategy for preparing hollow PI NPs through judicious selection of a suitable combination of PAA and an alternative porogen that exhibits a smaller value of $\Delta\delta$ (i.e., a more compatible pair). The phase-separated structure of the blend of PAA and the porogen is formed in the confined space within the PAA NPs, where the porogen remains in a dispersed state because of its high compatibility, leading ultimately to the formation of hollow cores after removal of the porogen. We have used these hollow PI NPs to assemble multilayered films having specific porous structures and, accordingly, reduced dielectric constants. Relative to the conventional template-assisted approach,[19−22] our proposed fabrication method is a simpler means of obtaining hollow PI NPs; furthermore, we suspect that it can be used to produce other types of hollow polymeric NPs.

Scheme 1

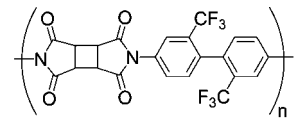

PI(CBDA-TFMB)

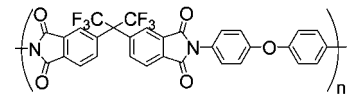

PI(6FDA-ODA)

Experimental Section

Materials. Two kinds of PIs were investigated (Scheme 1). PI(6FDA-ODA)[16] was synthesized from 4,4′-(hexafluoroisopropylidene)diphthalic anhydride (6FDA) and 4,4′-oxydianiline (ODA). PI(CBDA-TFMB)[9] was synthesized from 1,2,3,4-cyclobutanetetracarboxylic dianhydride (CBDA) and bis(2,2′-trifluoromethyl)benzidine (TFMB). Poly(methyl methacrylate) (PMMA; $M_w = 15\,000$) and poly(vinylpyrrolidone) (PVP; $M_w = 10\,000$) were used as porogens without further purification. 1-Methyl-2-pyrrolidinone (NMP; the good solvent), cyclohexane (the poor solvent), triethylamine (catalyst), and acetic anhydride (dehydrating agent) were purchased from Wako Pure Chemical Industries and used without further purification.

Preparation of Hollow/Multihollow PI NPs. A mixed NMP solution of the PAA and the porogen was prepared in the following manner. A given amount of an NMP solution of the porogen (1 wt %) was added to a diluted NMP solution of the PAA. The final concentration of the PAA was 1 wt %; the ratio of the added porogen to the amount of the PAA was varied from 0.05 to 0.8 in the NMP solution. In a typical reprecipitation[23,24] process, the mixed NMP solution (100 μL) of the PAA and the porogen was injected, using a microsyringe, into vigorously stirred cyclohexane (10 mL) at room temperature. A subsequent two-step imidization[14−17] was performed to convert the PAA to the PI. For chemical imidization, a mixture of triethylamine and acetic anhydride (1:1 molar ratio, 100 μL) was injected into the dispersion of the PAA NPs. After 5 h, the chemically imidized PI NPs were separated using a centrifuge, dried in vacuo, and then cured at 270 °C for 1 h to ensure complete conversion to the PI through thermal imidization.

(13) Zhao, G.-F.; Ishizaka, T.; Kasai, H.; Oikawa, H.; Nakanishi, H. *Mol. Cryst. Liq. Cryst.* **2007**, *464*, 613–620.
(14) Suzuki, M.; Kasai, H.; Miura, H.; Okada, S.; Nakanishi, H.; Oikawa, H.; Nihira, T.; Fukuro, H. *Mol. Cryst. Liq. Cryst.* **2003**, *406*, 151–157.
(15) Suzuki, M.; Kasai, H.; Ishizaka, T.; Miura, H.; Okada, S.; Oikawa, H.; Nihira, T.; Fukuro, H.; Nakanishi, H. *J. Nanosci. Nanotechnol.* **2007**, *7*, 2748–2752.
(16) Zhao, G.-F.; Ishizaka, T.; Kasai, H.; Oikawa, H.; Nakanishi, H. *Chem. Mater.* **2007**, *19*, 1901–1905.
(17) Zhao, G.-F.; Ishizaka, T.; Kasai, H.; Oikawa, H.; Nakanishi, H. *J. Nanosci. Nanotechnol.* **2008**, *8*, 3171–3175.
(18) Krevelen, D. W. V. *Properties of Polymers*; Elsevier: Amsterdam, 1990.
(19) Xu, X.; Asher, S. A. *J. Am. Chem. Soc.* **2004**, *126*, 7940–7945.
(20) Hu, Y.; Jiang, X.; Ding, Y.; Chen, Q.; Yang, C. Z. *Adv. Mater.* **2004**, *16*, 933–937.
(21) Wang, D.; Caruso, F. *Chem. Mater.* **2002**, *14*, 1909–1913.
(22) Meier, W. *Chem. Soc. Rev.* **2000**, *29*, 295–300.
(23) Kasai, H.; Nalwa, H. S.; Oikawa, H.; Okada, S.; Matsuda, H.; Minami, N.; Kakuta, A.; Ono, K.; Mukoh, A.; Nakanishi, H. *Jpn. J. Appl. Phys.* **1992**, *31*, L1132–L1134.
(24) Kasai, H.; Nalwa, H. S.; Okada, S.; Oikawa, H.; Nakanishi, H. In *Handbook of Nanostructured Materials and Nanotechnology*; Nalwa, H. S., Ed.; Academic Press: San Diego, CA, 1999; Vol. 5:Organics, Polymers, and Biological Materials.

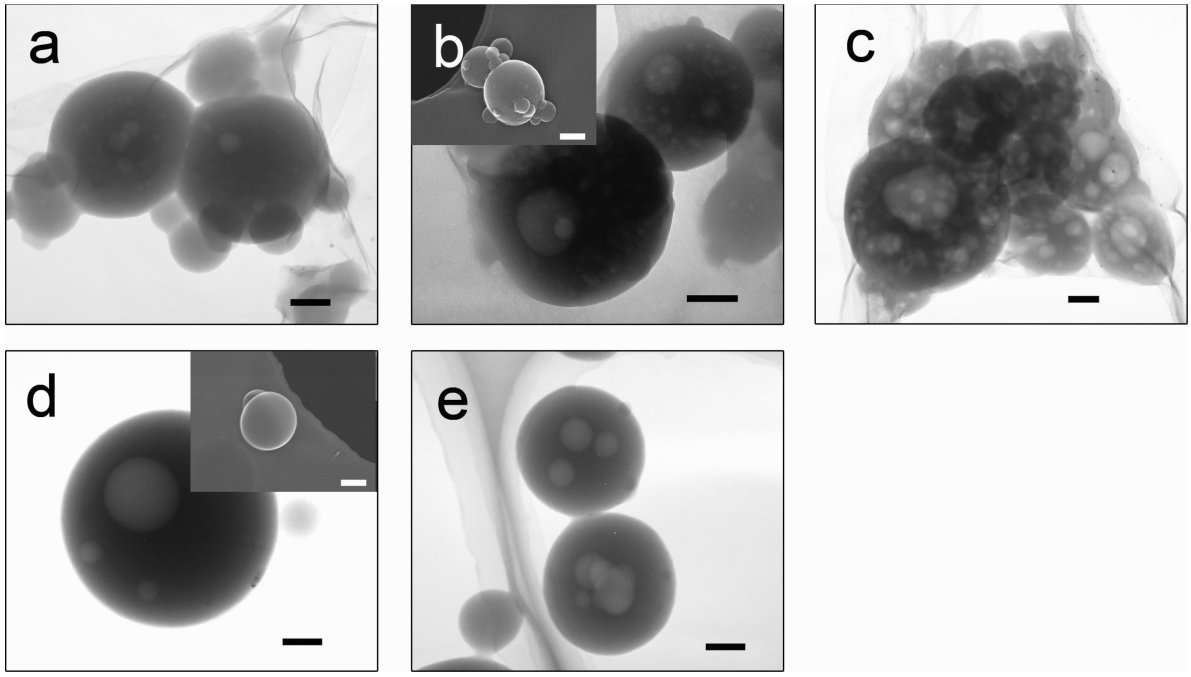

Figure 2. TEM images (scale bars: 100 nm) of multihollow PI(6FDA-ODA) NPs prepared using (a) PMMA 20 wt %, (b) PMMA 40 wt %, (c) PMMA 80 wt %, (d) PVP 20 wt %, and (e) PVP 40 wt %. The insets display corresponding SEM images (scale bars: 200 nm).

Table 1. Solubility Parameters[a] of the Materials Used in This Study

	solubility parameter ($MPa^{1/2}$)
PAA(CBDA-TFMB)	20.0
PAA(6FDA-ODA)	20.8
PVP	19.9
PMMA	19.7
cyclohexane	16.8
NMP	23.1

[a] Calculated using the Hoftyzer and van Krevelen method.[18]

Preparation of Multilayer Films of PI NPs. Electrophoretic deposition was performed according to the following procedure.[13,25−27] DC voltages (50−2000 V/cm) were applied to indium tin oxide (ITO) electrodes immersed in a face-to-face arrangement in a suspension of the PI NPs (solids concentration: 0.3, 0.5, 0.8, 1.5, or 2.0 wt %). The PI NPs were deposited onto the anode surface to form a multilayer film. The film was dried in air and then cured at 270 °C for 1 h to thermally imidize and pyrolyze the porogen. The electrophoretic deposition procedure was repeated to fill any cracks formed through coalescence of the NPs during the evaporation of the solvents.[13] The corresponding PAA solution (1 wt %, 100 μL) was then spin-coated (2500 rpm, 30 s) onto the resulting film. After thermal imidization, a multilayer PI NP film having a smooth surface was obtained. Pristine PI films were also prepared through thermal imidization of PAA films cast on a glass substrate.

Sample Characterization. Scanning electron microscopy (SEM) images were obtained using a JSM-6700F microscope (JEOL, Japan). Samples were prepared in the following manner. One droplet of each sample dispersion was placed onto a cleaned glass slide and air-dried at room temperature; the glass slide was fixed on the holder using double-faced carbon tape. The samples were coated with a thin Pt layer to increase the contrast and quality of the images, which were recorded at an acceleration voltage of 15 kV. Transmission electron microscopy (TEM) images were recorded using a JEOL JEM-2010 instrument operated at 200 kV. One droplet of the hollow PI NP dispersion was cast on a 150-mesh carbon-coated copper grid and air-dried at room temperature. Thermogravimetric analysis (TGA) was undertaken using a Perkin-Elmer Pyris 1 TGA apparatus operated at a heating rate of 10 K/min under a nitrogen atmosphere (50 mL/min). IR spectra were recorded using a ThermoNicolet AVATAR 360 FT-IR spectrometer. The capacitance (C_p) of each PI film was measured using an LCR meter (HIOKI 3535) operated in the frequency range from 100 kHz to 10 MHz under ambient atmospheric conditions. The dielectric constant k was calculated using the following equation:

$$k = \frac{tC_p}{Sk_0} \quad (1)$$

where t is the thickness of the sample, S is the area of the electrode, and k_0 is equal to 8.85×10^{14} C/m.

Results and Discussion

To demonstrate the applicability of our strategy, we prepared hollow/multihollow PI NPs using two different polymers as porogens. The initial PI that we evaluated for use as the matrix was PI(6FDA-ODA). Figure 2 reveals that multihollow PI NPs were formed when using PMMA as the porogen. Only a few small hollow cores (diameters: <20 nm) appeared inside the PI NPs after thermal imidization when the PMMA content was 20 wt % (Figure 2a). Upon increasing the PMMA content, larger hollow cores (diameters: ca. 100 nm), surrounded by several smaller cores, were generated; that is, the volume of the hollow structures increased accordingly (Figures 1a−c). In contrast, we obtained only larger hollow pores (fewer than five per NP) ranging in diameter from 100 to 200 nm when using PVP as the porogen. The number of hollow cores increased upon increasing the PVP content up to 40 wt %, but, due to high viscosity, agglomeration of the PAA NPs occurred at higher PVP contents (image not shown).

(25) Sarkar, P.; Nicholson, P. S. *J. Am. Ceram. Soc.* **1996**, *79*, 1987–2002.
(26) van der Biest, O. O.; Vandeperre, L. J. *Annu. Rev. Mater. Sci.* **1999**, *29*, 327–352.
(27) Besra, L.; Liu, M. *Prog. Mater. Sci.* **2007**, *52*, 1–61.

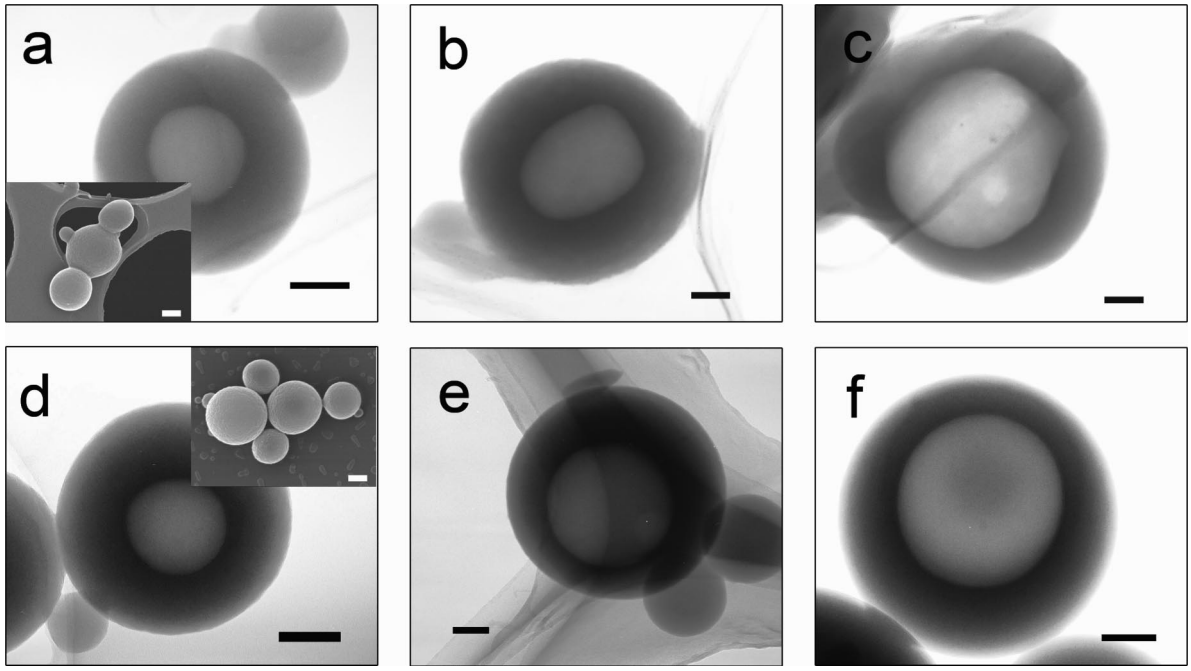

Figure 3. TEM images (scale bars: 100 nm) of hollow PI(CBDA-TFMB) NPs prepared using PMMA and PVP as porogens at contents of (a) PMMA 20 wt %, (b) PMMA 40 wt %, (c) PMMA 80 wt %, (d) PVP 20 wt %, (e) PVP 40 wt %, and (f) PVP 80 wt %. The insets display corresponding SEM images (scale bars: 200 nm).

Clearly, the selection of a suitable porogen is an important factor affecting the generation of hollow structures. A suitable porogen can be determined qualitatively by comparing its solubility parameter with that of PAA. The solubility parameter (Table 1) of PMMA ($\delta_{PMMA} = 19.7$) is closer to that of PAA(6FDA-ODA) ($\delta_{6FDA\text{-}ODA} = 20.8$) than it is to that of poly(acrylic acid) ($\delta_{PAS} = 23.6$), indicating that PMMA is more compatible with the former polymer. Such a relatively high compatibility decelerates the phase separation and causes the PMMA phase to remain within the PAA NPs, resulting in the formation of multihollow structures after the removal of the PMMA phase, rather than merely superficial pores. When we employed PVP ($\delta_{PVP} = 19.9$) as an even more compatible porogen for PAA(6FDA-ODA), the phase separation slowed down even further and the PVP phases remained to generate several large cores within the individual PI NPs. These findings indicate quite dramatically that the compatibility of the porogen and the PAA influences the number of hollow cores within the resulting PI NPs.

The selection of a suitable porogen for a specific PAA allows the formation of a single hollow core within each PI NP. Our approach is also applicable to other PAAs—as long as they can dissolve in the solvent. The second PI that we evaluated was PI(CBDA-TFMB) ($\delta_{CBDA\text{-}TFMB} = 20.0$). Interestingly, the TEM images in Figure 3 reveal only one type of hollow morphology formed—namely, a single hollow core—when using either PMMA or PVP as the porogen at contents greater than 40 wt %. Because these porogens are more compatible with PAA(CBDA-TFMB) than with PAA(6FDA-ODA), the phase separation decelerated and the porogen phase integrated into a single domain, which ultimately formed the single hollow core. Figure S1 (Supporting Information) presents a plausible mechanism for the formation of these hollow PI NPs. Moreover, the diameters

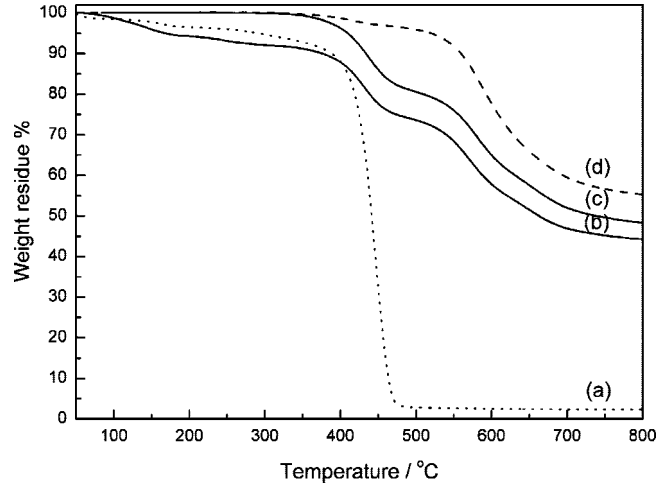

Figure 4. TGA (weight loss) curves of (a) PVP, (b) chemically imidized hollow PI(6FDA-ODA) NPs, (c) thermally imidized hollow PI(6FDA-ODA) NPs, and (d) PI(6FDA-ODA) NPs. The PVP content was 20 wt % in (b) and (c).

of the hollow cores increased upon increasing the content of added PVP/PMMA. At 80 wt %, we prepared hollow PI NPs possessing core diameters in the range 200−400 nm—the highest degree of porosity obtained in this present study. The chemical structure of the PAA precursor clearly affected the hollow morphology of the resulting PI NPs. Nevertheless, PMMA and PVP were both effective porogens for the two PAA derivatives.

We used TGA to measure the thermal behavior of the resulting hollow/multihollow PI NPs (Figure 4). PVP began to decompose at ca. 200 °C (TGA curve a). The chemically imidized hollow PI(6FDA-ODA) NPs also exhibited weight loss at ca. 200 °C (TGA curve b), probably due to the pyrolysis of residual PVP and solvent. This finding implies

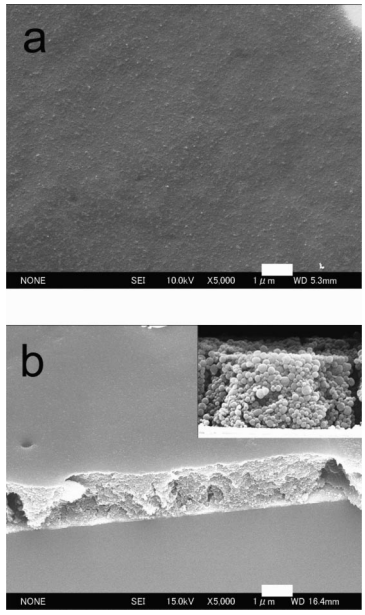

Figure 5. (a) Surface and (b) cross-sectional SEM images of a typical porous PI film assembled from PI(CBDA-TFMB) NPs. The inset displays a magnified view. Scale bars: 2 μm.

the existence of a PVP phase within the PI NPs after chemical imidization. Indeed, we observed (TEM) such PVP phases within composite NPs of PAA and porogen prior to thermal imidization (Figure S2, Supporting Information). In contrast, the thermally imidized hollow PI NPs (TGA curve c) were thermally stable up to 300 °C, with a 5%-weight-loss temperature of 400 °C. This thermal stability was almost identical to that of the ordinary PI NPs (TGA curve d), suggesting that little, if any, PVP remained within the thermally imidized hollow PI NPs; that is, the hollow PI NPs were formed through thermal decomposition of the microphase-separated porogen within the composite PI/porogen NPs. The IR spectra of the hollow PI NPs (Figure S3, Supporting Information) were consistent with the TGA results.

We employed electrophoretic deposition to assemble the resultant hollow PI NPs into multilayered films of type C (Figure 1). An applied DC field caused the negatively charged PI NPs (dispersed in cyclohexane) to move toward and become deposited on the anode. After performing the electrophoretic deposition twice, we obtained crack-free and continuous films over a large area. Subsequent spin-coating and thermal treatment processes led to the PI NPs being attached to their neighboring NPs, providing uniform and densely packed films of assembled PI NPs (Figure 5). We controlled the thickness of the films within the range from 500 nm to 10 μm by changing either the concentration of the dispersion or the applied voltage (Figure S4, Supporting Information). The dielectric constants of these porous PI films were governed by the intrinsic dielectric constant of the PI, the degree of porosity of the PI NPs, and the multilayer morphology. Figure 6 presents the relationship between the dielectric constant and the morphology of the PI film. The dielectric constants of the pristine PI films (Type A, Figure 1) cast from PI(CBDA-TFMB) and PI(6FDA-ODA) were 2.5 and 2.8, respectively. The dielectric constants of multilayer films of PI NPs of type B were somewhat lower. The degree of porosity of the type B films was only approximately 16% (calculated from a N_2 adsorption study), significantly lower than that expected for rhombohedral dense packing of spherical NPs. We suspect that the wide dispersity of the PI NPs and their attachment to neighboring PI NPs were responsible for such poor porosity. The dielectric constants decreased significantly upon increasing the degree of porosity of the PI films from type B to type C, that is, using hollow PI NPs instead of PI NPs. Amazingly, the dielectric constant was ca. 1.9 for the multilayer films formed from the hollow PI(CBDA-TFMB) NPs. This dielectric constant is even lower than that of a cast film of poly(tetrafluoroethylene), which has the lowest dielectric constant among the known polymeric insulators. Thus, the introduction of air pores within the PI NPs reduced the dielectric constant significantly. We measured the dielectric constants through each film at more than 20 points, with no great differences observed, suggesting uniformity and continuity throughout the porous PI films. For their use as interlayer dielectrics, PI films should also exhibit thermal stability and excellent mechanical properties. The TGA results in Figure 4 suggest that the hollow PI NPs were stable at temperatures up to 400−450 °C, depending on the type of pristine PI; that is, the resultant films of hollow PI NPs exhibited very high thermal stability. In addition, the multilayered films of hollow PI NPs survived the Scotch tape test. Releasing the substrate through dipping in dilute hydrochloric acid provided free-standing films, but they were not particularly robust. Nevertheless, we suspect that the mechanical properties might improve if additional attachments were to form between the individual hollow PI NPs during thermal treatment.

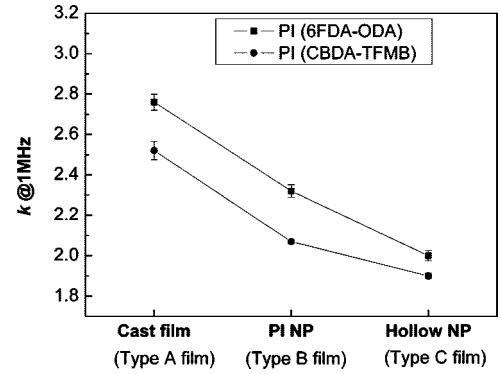

Figure 6. Dielectric constants of PI films exhibiting various porous morphologies: Cast film, pristine PI films (Type A films); PI NP, multilayered films assembled from PI NPs (Type B films); hollow NP, multilayered films assembled from hollow PI NPs (Type C films). Film types A−C are illustrated in Figure 1.

Conclusion

We have successfully prepared hollow/multihollow PI NPs using the reprecipitation method with PVP and PMMA as porogens. The hollow pores, ranging in diameter from 20 to 400 nm, were induced through (i) microphase separation of PAA and the porogen and (ii) subsequent pyrolysis of the porogen during thermal imidization. The morphologies of the pores were affected primarily by the compatibility of the

PAA and the porogen. The unique hollow morphologies of these PI NPs make them alternative candidates for use in dielectric interlayer applications as well as in the design of catalyst supports, reaction vessels, and biocompatible nanodevices possessing tailored internal nanostructures. Our strategy illustrated in Figure 1 is an effective means for preparing ultralow-k PI films featuring unique porous structures. We obtained a particularly low dielectric constant (k = ca. 1.9) for a multilayer film assembled from one such type of hollow PI NPs. Currently, we are investigating the mechanical properties of the films and modifying the fabrication process in an attempt to improve their mechanical properties and, thereby, satisfy the requirements for their use as interlayer dielectrics.

Supporting Information Available: A plausible mechanism for the formation of hollow PI NPs; TEM images of PAA NPs without thermal imidization; IR spectra of hollow PI NPs; and thicknesses of PI films plotted with respect to the fabrication conditions (PDF). This material is available free of charge via the Internet at http://pubs.acs.org.

CM802989U